Korean J. Chem. Eng., **29**(3), 396-403 (2012)
DOI: 10.1007/s11814-011-0175-5

Separation of sinigrin from Indian mustard (*Brassica juncea* L.) seed using macroporous ion-exchange resin

Tianxin Wang, Hao Liang, and Qipeng Yuan†

State Key Laboratory of Chemical Resource Engineering, Beijing University of Chemical Technology, Beijing 100029, China
(*Received 28 September 2010 • accepted 6 July 2011*)

Abstract–Sinigrin is a major glucosinolate present in Indian mustard (*Brassica juncea* L.) seeds as the precursor of the anticancer compound allyl isothiocyanate. In the present study, the adsorption and desorption characteristics of six macroporous ion-exchange resins for the separation of sinigrin from crude aqueous extracts have been compared. The results indicated that D261 resin showed the best adsorption and desorption capacity to sinigrin, and its adsorption data fit best to the Freundlich isotherm. The dynamic adsorption/desorption experiments were carried out to optimize the separation process. After treatment with D261 resin in one run, the purity of sinigrin in the product was increased 15.57-fold from 3.75% to 58.37% with the recovery of 79.82%. Meanwhile, the separation effect of D261 resin was also supported by UV and IR. The separation process using macroporous ion-exchange resin in our paper provides a novel, rapid and economical method for separation of sinigrin.

Key words: Sinigrin, Indian Mustard, *Brassica juncea* L., Macroporous Ion-exchange resin, Separation

INTRODUCTION

The available scientific evidence suggests that risk for developing cancer probably is reduced by an increasing consumption of diets high in vegetables and fruits [1]. Mustards belonging to the family *Brassicaceae* are widely consumed by humans [2]. Sinigrin (Fig. 1), 2-propenyl or allyl glucosinolate, is a major glucosinolate present in Indian mustard (*Brassica juncea* L.) seeds as the precursor of the myrosinase-mediated breakdown product allyl isothiocyanate [3], which possesses many biological activities such as bactericidal, antibacterial activities [4,5], and plays an important role in preventing cancer and DNA damage, caused by carcinogens in the diet effectively [6,7]. When ingestion of mustards, though myrosinase is inactivated by cooking, sinigrin still could reach the large intestine, where resident microflora mediate the formation of biologically active isothiocyanate [8]. Thus, sinigrin could be added to functional food as phytochemical component of healthy diets to achieve its conversion to biologically active compounds in the alimentary tract automatically.

Glucosinolates are a class of water-soluble compounds because of their ionized sulfate and hydrophilic thioglucose moieties. Due to their physicochemical properties, separation and purification become extremely difficult [9]. A number of approaches to isolating some glucosinolates from plant materials have been documented, including alumina column chromatography [10], preparative high-speed counter-current chromatography [11], preparative high performance liquid chromatography [12], strong ion-exchange centrifugal partition chromatography [13] and slow rotary counter-current chromatography [9]. Though these techniques have been applied to separate and purify some glucosinolates in order to obtain the standards, they still couldn't satisfy the increasing market demand of sinigrin. Moreover, these methods are not effective regarding precise instruments, a large amount of high-salt and highly polar reagents, massive energy consumption and intensive labor. Therefore, an alternative approach to scale up in order to obtain the product for commercial use becomes necessary.

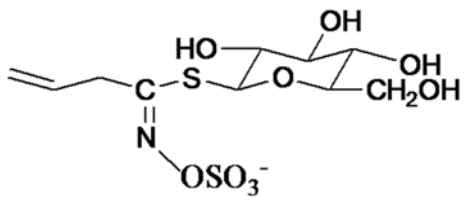

Fig. 1. Chemical structure of sinigrin.

The adsorption/desorption process of macroporous ion-exchange resin is an efficient method for primary separation and concentration that has been widely used in the field of food, pharmaceutical and environment industries [14-19]. Macroporous ion-exchange resin is characterized by a permanent well developed porous structure and its functional group. Due to its high degree of cross linking, it is resistant to degradation caused by osmotic shock and oxidation [20,21]. Furthermore, its adsorption effect is determined by its functional group predominantly. The functional group intensifies macroporous ion-exchange resin to adsorb ionized target molecules from polar solution, which is quite suitable for the charged hydrophilic glucosinolates. And macroporous ion-exchange adsorption/desorption is an environment-friendly technique using water and salt as the only reagents in the whole operating process. Compared to conventional separation methods, the adsorption/desorption method is superior, because of its procedural simplicity, low cost, high efficiency and security [22], so it may provide scientific references for the large-scale production.

†To whom correspondence should be addressed.
E-mail: yuanqp@mail.buct.edu.cn

Among various plant in the family *Brassicaceae*, Indian mustard seeds rich in sinigrin appear to be a good resource for separation and purification [23]. In our study, the properties of adsorption and desorption of sinigrin on different macroporous ion-exchange resins have been investigated. Certain parameters such as pH value of the sample, the temperature, the concentration of the sample, the concentration and flow rate of the desorption solution, were also studied to ensure the separation efficiency. The result could be referred for separation of sinigrin from Indian mustard seeds.

EXPERIMENTAL SECTION

1. Materials and Reagents

Indian mustard (*Brassica juncea* L.) seeds were purchased from Anhui Fangmin Medicine Co., Ltd. (AnHui, China). Sinigrin standard was purchased from AppliChem Company (Darmstadt, Germany). Methanol and trifluoroacetic acid (TFA) from Dikma Technologies Inc. (California, USA) were HPLC-grade. Petroleum ether and methanol from Beijing Chemical Works (Beijing, China) were analytical-grade. Deionized water was purified by a Milli-Q water purification system (Bedford, Massachusetts, USA). All solutions prepared for HPLC were filtered through 0.45 μm nylon membranes before being used.

2. Adsorbents

Macroporous ion-exchange resins including strongly basic anion-exchange resins D201, D296, D261 and weakly basic anion-exchange resins D301, D311, D380 were purchased from Anhui Sanxing Resin Technology Co., Ltd. (Anhui, China) and Tianjin Nankai Hecheng S&T Co., Ltd. (Tianjin, China). The physical properties of macroporous ion-exchange resins are summarized in Table 1. These macroporous resins were pretreated with 3% HCl and NaOH solutions successively to remove the monomers and porogenic agents trapped inside the pores during the synthesis process, and subsequently the HCl or NaOH was thoroughly replaced with pure water.

3. Preparation of Crude Plant Extract

Indian mustard seeds were heated to inactivate myrosinase under 100 °C for 2 h, and then were homogenized in a grinder. Ground seed meals were defatted with petroleum ether, then stirred for 30 min in a 10-fold excess (w/v) of boiling water three times. After the supernatant was filtered, the extracted solution was concentrated and dissolved in a measured volume of deionized water for quantitative analysis by HPLC.

4. HPLC Analysis of Sinigrin

Quantification of sinigrin concentration was carried out by a Shimadzu HPLC apparatus equipped with Shimadzu model LC-20AT pumps, an LC-20A UV detector, a SEDEX 75 ELSD detector (Sedere, France), a CTO-10ASVP column oven (Shimadzu, Kyoto, Japan), and a reversed-phase C18 column (250 mm×4.6 mm, 5 μm, Dianmonsil™, USA). The column temperature was maintained at 30 °C. The elution started of 1.0% v/v methanol/water (0.1% v/v TFA), then methanol was raised to 70% during 20 min and maintained for 2 min to purge the column. The flow rate employed was 1.0 mL/min throughout the run. 5 μL samples were injected into the column. The UV detector was set at 235 nm and the ELSD detector was set at 40 °C and 3.5 kPa.

5. Static Adsorption and Desorption Tests

The static adsorption tests of Indian mustard extracts were carried out as follows: 1.0 g test resin was put into flask with a lid, then 25 mL sample solution of sinigrin extracts was added. The flask was then shaken at 110 rpm for 12 h at a constant temperature of 20 °C. The solutions before and after adsorption were analyzed by HPLC.

The static desorption process was conducted as follows: after adsorption equilibrium was reached, the resins were first washed by deionized water and then desorbed with 25 mL 1.0 mol/L KCl aqueous solution. The flask was shaken at 110 rpm for 12 h at a constant temperature of 20 °C. The desorption solution was analyzed by HPLC.

The preliminary choice of resins was evaluated by their capacities of adsorption, and their ratios of adsorption and desorption. The adsorption and desorption properties under different conditions including pH value of the sample and salt concentration used for desorption were also compared. The adsorption isotherms of sinigrin on selected resin at different temperatures (20 °C, 30 °C and 40 °C) were also studied. Their Langmuir and Freundlich equations were evaluated.

6. Dynamic Adsorption and Desorption Tests

Dynamic adsorption and desorption experiments were carried out in a glass column wet-packed with the selected resins. Sample solution flowed through the glass column at a certain concentration, and sinigrin concentration was monitored by HPLC analysis. While adsorptive equilibration, the adsorbate-laden column was washed with deionized water first, then eluted by a certain concentration of KCl aqueous solution at a certain flow rate. Sinigrin concentration in the eluent was analyzed by HPLC. The effects of initiate concentration of the sample, the salt concentration and flow rate of the desorption solution on the capability of adsorption and desorption were studied, respectively.

7. Calculation of the Adsorption Capacity, the Ratios of Adsorption and Desorption

The following equations were used to quantify the capacity of

Table 1. Physical properties of the macroporous ion-exchange resins used

Type	Particle diameter (mm)	Moisture content (%)	Exchange capability (mM/g resin)	Density (g/mL)	Surface functional group
D201	0.300-1.25	65-75	3.7	1.05-1.12	$-N^{+}(CH_3)_3$
D261	0.315-1.25	50-60	3.6	1.06-1.13	$-N^{+}(CH_3)_3$
D296	0.315-1.25	50-60	3.6	1.05-1.10	$-N^{+}(CH_3)_3$
D301	0.315-1.25	50-60	4.8	1.03-1.07	$-N(CH_3)_2$
D311	0.315-1.25	58-65	7.0	1.07-1.12	$-N(CH_3)_2$
D380	0.315-1.25	70-73	6.5	1.04-1.05	$-NH_2$

adsorption, as well as the ratios of adsorption and desorption.

Adsorption capacity:

$$q_e = \frac{(C_0 - C_e) \times V}{m_S} \quad (1)$$

Adsorption ratio:

$$E = \frac{C_0 - C_e}{C_0} \times 100\% \quad (2)$$

Where the q_e (mg/g) is the adsorption capacity, which represents the mass of adsorbate adsorbed on 1 g resin at adsorption equilibrium point; E is the adsorption ratio (%), which means the percentage of adsorbate adsorbed at adsorption equilibrium point; C_0 and C_e are the initial and equilibrium concentration of sinigrin in solutions, respectively (mg/mL), V is the volume of the sample solution (mL), m_s is the mass of the resin (g).

Desorption ratio:

$$D = \frac{C_d \times V_d}{(C_0 - C_e) \times V} \times 100\% \quad (3)$$

Where D is the desorption ratio (%), C_d is the concentration of sinigrin in the eluent (mg/mL), V_d is the volume of the eluent (mL), C_0, C_e and V are the same as defined above.

8. Fourier Transform Infrared (FTIR) Characterization

The FTIR spectra were recorded from pressed discs of original, adsorbed and desorbed macroporous ion-exchange resins using a Fourier Transform IR Affinity-1 Spectrophotometer (Shimadzu, Kyoto, Japan) as KBr pellets in the range of 4,700-340 cm^{-1}, averaging the data of 40 successive scans. The functional groups of macroporous ion-exchange resins were characterized. Meanwhile, the standard of sinigrin (solid form) and the extracts of Indian mustard seeds before and after treatment of resins (solid form) were also analyzed. The spectra interpretation was performed using reference information [24].

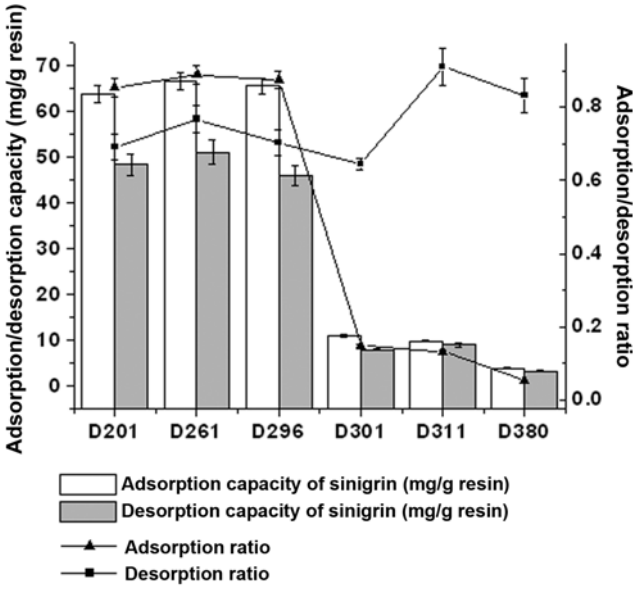

Fig. 2. Results of adsorption and desorption capacity, the ratios of adsorption and desorption of different macroporous anion-exchange resins towards sinigrin.

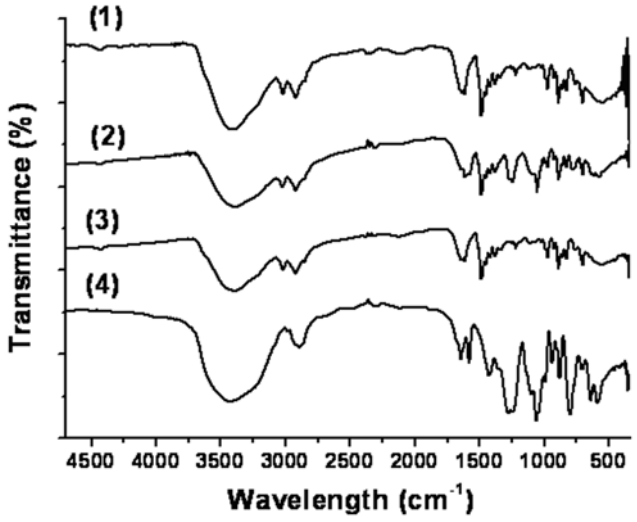

Fig. 3. IR spectra of (1) original D261 resin; (2) D261 resin after adsorption; (3) D261 resin after desorption; (4) the standard of sinigrin.

RESULTS AND DISCUSSION

1. The Adsorption Capacity, Ratios of Adsorption and Desorption

Six macroporous anion-exchange resins with different physical properties were employed for separation of sinigrin, and the results are listed in Fig. 2. The adsorption and desorption capacity of sinigrin on macroporous strongly basic anion-exchange D261, D201, D296 resins was much better than that on macroporous weakly basic anion-exchange resins. The excellent adsorption capacity of macroporous strongly basic anion-exchange D261 resin towards sinigrin could be associated with its functional group ($-N^+(CH_3)_3$). The functional groups of original, adsorbed and desorbed D261 resins were characterized by FTIR and the spectra are displayed in Fig. 3. The $-N^+(CH_3)_3$ group exhibits the distinctive spectral band (~885-900 cm^{-1}) in the wavelength range investigated, and the presence of the quaternary nitrogen in the resin is also clearly indicated by the vibrations of O-H bonded to the charged nitrogen $N^+(CH_3)_3 \cdots OH^-$. Before the adsorption, a strong and broad band in the 3,500-3,300 cm^{-1} region (O-H stretching vibration) and a band at 1,640 cm^{-1} (O-H bending vibration) indicated the presence of coordinated water molecules associated with these ionic pairs, with the peak at 975 cm^{-1} (O-H deformation vibration) indicating the presence of hydroxyl. Then after adsorption, the peaks at 975 cm^{-1}, 1,640 cm^{-1} and 3,300-3,500 cm^{-1} weakened significantly. The decreasing tendency of these three peaks indicated that most of the hydroxyl groups were replaced by adsorbed sinigrin [24,25]. The peaks appearing at 1,270 cm^{-1}, 1,245 cm^{-1} and 1,060 cm^{-1} were attributed to the vibration of adsorbed sinigrin, compared with the standard of sinigrin. Moreover, after desorption, these distinctive peaks of sinigrin disappeared. Thus, it could be concluded that strongly basic anion-exchange D261 resin exhibited its possible procedure of adsorption and desorption of ionized sinigrin as shown in Fig. 4. Additionally, our batch adsorption experiments indicated that when D261 resin was mixed with extracts, the solution pH increased from 5.6 to 9.2, indicating the release of OH^- anions. When D261 resin was mixed with water, the solu-

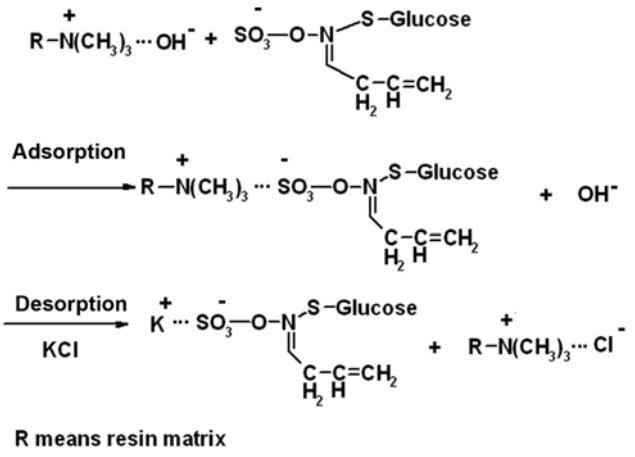

Fig. 4. Procedure of adsorption and desorption of sinigrin using macroporous strongly basic anion-exchange D261 resin.

tion pH slightly increased from 7.2 to 7.8. These results were similar to that reported by Wang et al. The adsorption of pertechnetate (TcO_4) can be associated with the binding site R-C-OH, where R represents aromatic rings. Pertechnetate is adsorbed on the R-C-OH site by displacing the hydroxyl group as described in reaction R-C-OH+ $TcO_4^- \rightarrow$R-C-OTcO_3+OH^- [26]. The results above also supported the proposed adsorption procedure shown in Fig. 4. Considering the adsorption capability and the ratios of absorption and desorption, the optimal macroporous ion-exchange resin D261 was selected to further investigate adsorption/desorption behavior towards sinigrin.

2. Effect of pH Value on the Capacity of Adsorption

The pH value influenced the extent of ionization of target molecules, thereby affecting their adsorption affinity [27]. Hydrogen bonding plays an important role in the adsorption/desorption process of macroporous resins. At higher pH values, the hydrogen bonding interactions between flavonoids and resins with polar functional groups, such as acylamino and phenolic hydroxyl groups, are reduced, because the phenolic hydroxyl groups in flavonoids and resins dissociate to form H^+ and their corresponding anions, resulting in the decrease of adsorption capacity and adsorption ratio [28]. For D261 ion-exchange resin selected, the adsorption capabilities at different pH values were nearly the same (Table 2). The pH value of the extracts had insignificant effect on the efficiency of adsorption ($p>0.05$). It can be explained by the different interaction between macroporous ion-exchange resins and substrate, compared with that between non-ionized macroporous resins and substrate. In a wide pH range, the high degree of ionic interaction still existed between the sulfate part $-SO_3^-$ of sinigrin and the functional group $-N^+(CH_3)_3$ of resins, which was not influence by the pH alteration. It also proved that the ionization of functional group and sinigrin played a predominantly important role in the adsorption process of D261 resin. Finally, natural pH value of 5.63 was selected for the following tests to simplify the process.

Table 3. Langmuir and Freundlich adsorption parameters of sinigrin on anion-exchange D261 resin at different temperatures

	20 °C	30 °C	40 °C
Langmiur model			
Equation	$q_e=\frac{1999.96C_e}{1+31.60C_e}$	$q_e=\frac{1428.77C_e}{1+22.14C_e}$	$q_e=\frac{999.88C_e}{1+14.00C_e}$
R^2	0.9768	0.9806	0.9676
q_0 (mg/g)	63.29	64.52	71.42
K	31.60	22.14	14.00
Freundlich model			
Equation	$q_e=124.92C_e^{\frac{1}{2.244}}$	$q_e=121.37C_e^{\frac{1}{2.104}}$	$q_e=138.68C_e^{\frac{1}{1.802}}$
R^2	0.9969	0.9959	0.9696
K_f (mg/g)	124.92	121.37	138.68
1/n	0.4457	0.4752	0.5550

3. Adsorption Isotherms

Equilibrium adsorption isotherms on D261 resins at different temperatures were obtained by contacting 25 mL aqueous solution of sinigrin crude extracts with D261 resin. The Langmuir and Freundlich equations are used to reveal the linearity fitting and interaction of solutes with the resins. They are the most popular ones frequently used in description of the experimental data of adsorption isotherms, because of their relative simplicity and reasonable accuracy [29]. The Langmuir equation describes the adsorption behavior of monomolecular layer, while the Freundlich equation is used extensively in the physical and chemical adsorption, which can be used to describe the adsorption behavior of monomolecular layer as well as that of the multimolecular layer.

The experimental data were fitted to the Langmuir equation:

$$q_e=\frac{q_0KC_e}{1+KC_e} \quad (4)$$

Where K is the adsorption equilibrium constant and q_0 is the empirical constant.

The experimental data were also fitted to the Freundlich equation:

$$q_e=K_fC_e^{1/n} \quad (5)$$

Where K_f is the Freundlich constant that is an indicator of adsorption capacity, and 1/n is an empirical constant related to the magnitude of the adsorption driving force [30].

The Langmuir and Freundlich parameters are summarized in Table 3. We can see that the correlation coefficients of both Langmuir and Freundlich equations on D261 resin were rather high, and its adsorption data fit best to the Freundlich isotherm which could describe the better adsorption behavior of sinigrin on D261 resin. It indicated that each site of the adsorbent could adsorb not only one layer. In the Freundlich equation, the adsorption can take place easily when

Table 2. Effect of different pH value of sample solution on the adsorption ratio of D261 resin towards sinigrin

pH	2	4	6	8	10
Adsorption capacity (mg/g)	55.27±1.82	57.03±1.62	58.36±1.91	58.16±2.14	56.52±1.53
Adsorption ratio (%)	87.73±2.89	90.52±2.57	92.63±3.03	92.31±3.40	89.71±2.43

the 1/n value is between 0.1 and 0.5, and it is not easy to happen if 1/n value is between 0.5 and 1; however, it is very difficult to occur if 1/n value exceeds 1 [31]. In Table 3, the 1/n values were between 0.40 and 0.60, which indicated that the D261 resin was appreciated for separating sinigrin. Moreover, the results clearly exhibited that the maximum adsorption increased with the temperature increasing. It suggested that low temperature restricted the occurrence of adsorption and the present adsorption was endothermic.

4. Adsorption Kinetics on D261 Resin

Adsorption kinetics curve was obtained for sinigrin on D261 resin at 20 °C (Fig. 5), the adsorption capacity increased with the extension of adsorption time, and quickly reached the equilibrium at 50 min. The adsorption behavior may be consistent with Freundlich multimolecular layer adsorption and the strong interaction between the functional group $-N^{+}(CH_3)_3$ of D261 resin and $-SO_3^{-}$ part of sinigrin. The fast adsorption process suggested that we might choose a high flow rate during the dynamic adsorption process.

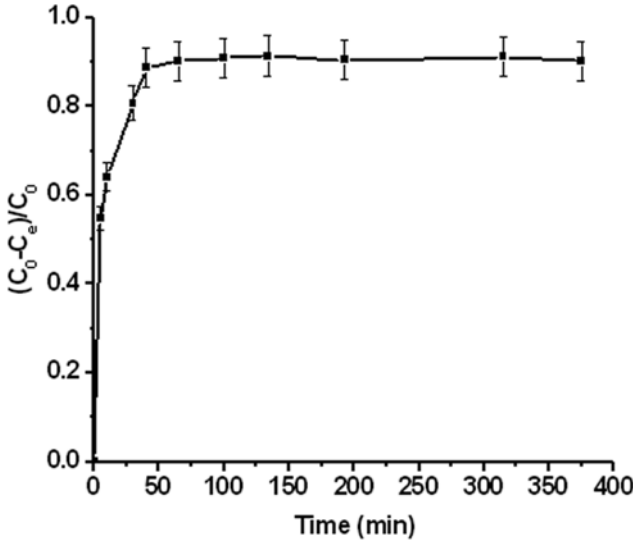

Fig. 5. Adsorption kinetic curve of sinigrin onto D261 resin at 20 °C.

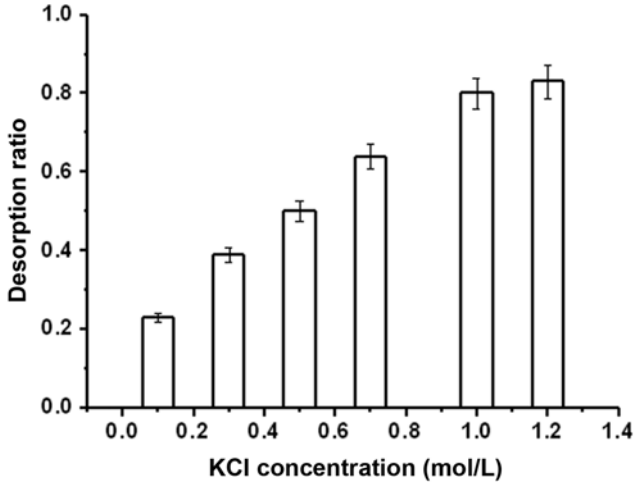

Fig. 6. Effect of different concentration of KCl on the static desorption ratio of sinigrin on D261 resin at 20 °C.

5. Static Desorption on D261 Resin

The proper desorption solution was chosen according to the ionization of resins and the sinigrin solubility in the desorption solution. Sinigrin could be dissolved easily in KCl aqueous solution. In addition, as shown in Fig. 6, the desorption ratio of sinigrin increased with the KCl concentration increasing. However, there is no significant difference between those of the KCl concentration of 1.0 mol/L and 1.2 mol/L at $p>0.05$. The maximum desorption ratio was found to be 80.58%, when using KCl at the concentration of 1.0 mol/L. Therefore, 1.0 mol/L KCl aqueous solution was selected as the appropriate desorption solution.

6. Dynamic Adsorption and Desorption on D261 Resin

The results of dynamic adsorption are summarized in Table 4. The highest adsorption capacity was observed when the initial concentration of sinigrin was 0.464 mg/mL. The adsorption capacity decreased with initial concentration increasing, maybe due to the competition to the active sites of D261 resin between sinigrin and impurities in the crude extracts and the limitation of diffusivity of sinigrin into the micropores of D261 resin. However, the lower initial concentration prolonged the working time and increased the sample volume. Thus, considering the working time and the adsorption capacity, 2.0 mg/mL was selected for the further step.

Different concentrations of KCl aqueous solutions (0.1, 0.5, 1.0

Table 4. Breakthrough volumes and adsorption capacity of sinigrin on D261 resin at different sample concentrations under dynamic adsorption conditions

Initial concentration (mg/mL)	Breakthrough point (BV)	Mass of sinigrin adsorbed (mg)	Adsorption capacity (mg/g resin)
0.464	69	320.16	64.03
1.546	20	309.20	61.84
2.037	15	305.55	61.11
2.355	12	282.60	56.52

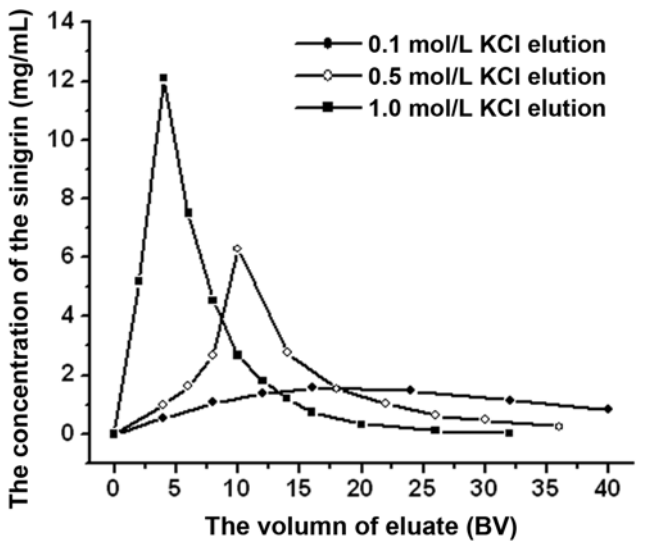

Fig. 7. Effect of different concentration of desorption solution under the dynamic desorption condition of sinigrin on D261 resin at 20 °C.

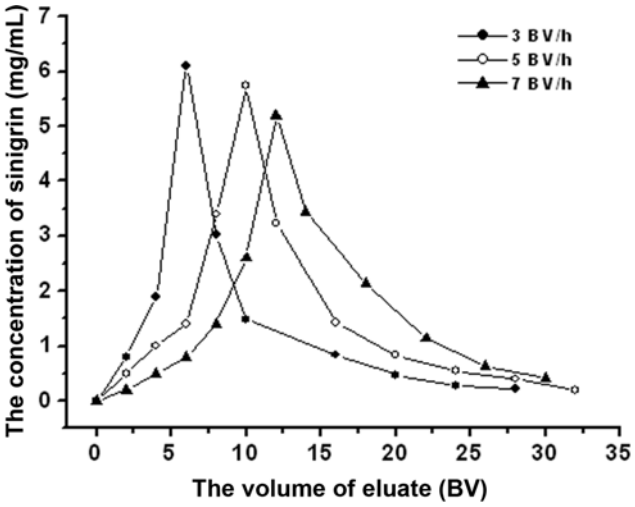

Fig. 8. Dynamic desorption curves of sinigrin on column packed with D261 resin at different desorption flow rates.

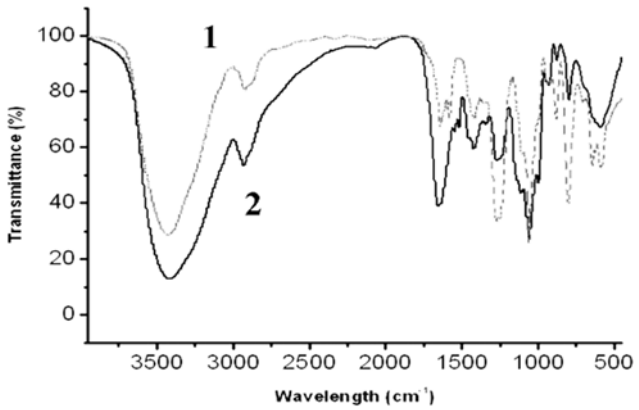

Fig. 10. IR spectra of sample solution after (1) and before (2) treatment with D261 resin.

mol/L) were used to perform desorption tests in order to choose proper desorption solution. As shown in Fig. 7, with the KCl concentration increasing, the desorption ratio was increased. 0.1 mol/L KCl aqueous solution nearly couldn't elute sinigrin from the D261 resin, while 1.0 mol/L KCl aqueous solution could reach the maximum desorption ratio over 80%. Thus, 0.1 mol/L KCl aqueous solution could be used to remove the impurities and pigments with little loss of sinigrin, and 1.0 mol/L KCl aqueous solution was selected as the appropriate desorption solution and used in the dynamic desorption experiments. It is also very important to choose a proper flow rate in order to desorb sinigrin from resins effectively. As seen in Fig. 8, during the dynamic desorption tests, the desorption performance at slow flow rate was better. Lower volume was consumed and more narrow range of elution was exhibited. Therefore, 3 BV/h was selected as the proper desorption flow rate in consideration of the lower volume consumption.

After dynamic adsorption and desorption experiments were carried out in the glass column wet-packed with the selected D261 resin, the optimum parameters were obtained: the concentration of sample solution 2.0 mg/mL, pH value 5.63, the flow rate 3 BV/h for adsorption; KCl aqueous solution (0.1 mol/L) and followed by KCl aqueous solution (1.0 mol/L) as the desorption solution, and the flow rate 3 BV/h for desorption.

In addition, the effect of D261 resin on separating singrin was examined by UV, IR and ELSD-HPLC. Fig. 9 showed the HPLC chromatograms between raw water extraction and the eluete. In the UV spectra, it can be seen that some impurities of characteristic absorption band of 325 nm were removed by D261 resin. By HPLC-ELSD, the number of constitutes contained in the solution was significantly decreased from 8 to 3, which exhibited that macroporous ion-exchange resin could separate the sinigrin, efficiently; then the content of KCl (32.5%) and the content of sinigrin (58.37%) were determined. The existence of monovalent KCl was the key factor influencing the purity of the product. In our laboratory, glucoraphenin (4-methylsulfinyl-3-butenyl glucosinolate), another aliphatic glu-

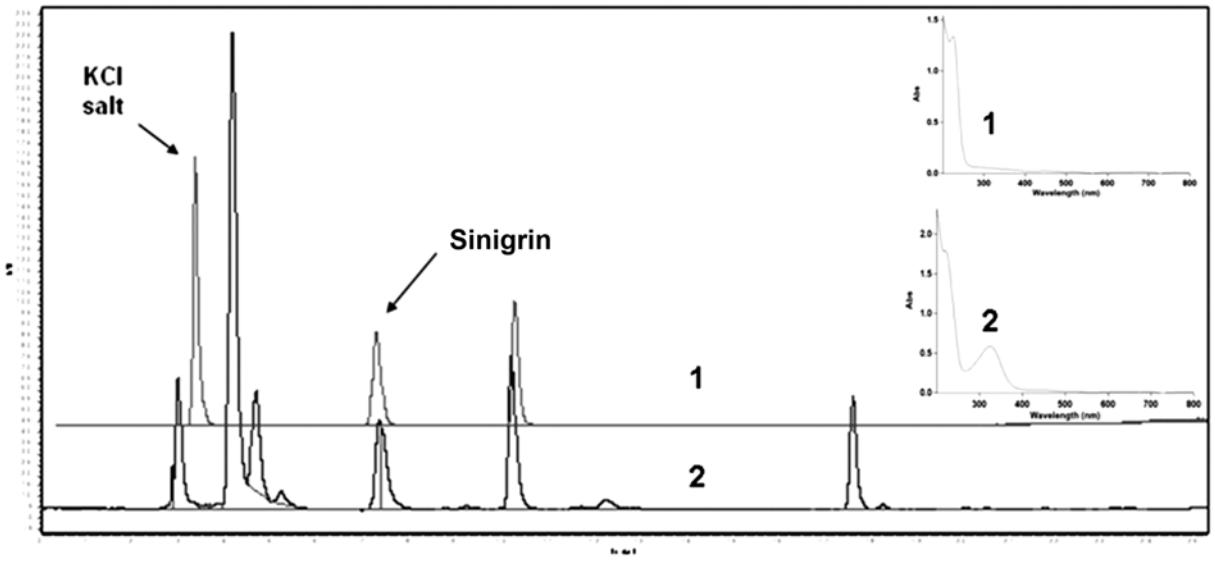

Fig. 9. HPLC and UV spectra of sample solution after (1) and before (2) treatment with D261 resin.

cosinolate, was successfully separated from the KCl solution using nanofiltration membrane [32]. Thus, the nanofiltration technology will become a promising method applied to remove the KCl in our further section. Meanwhile, the IR spectra showing the locations of characteristic functional groups of the two samples are compared in Fig. 10. There are significant increases at the characteristic wavelength of sinigrin, such as 800.4 cm^{-1} ($\omega_{C=C}$) and 878.2 cm^{-1} (γ_{N-O}), which suggests that sinigrin was separated and concentrated through the adsorption/desorption process using D261 macroporous ion-exchange resin.

CONCLUSIONS

The separation process of sinigrin with macroporous ion-exchange resin has been successfully developed in this study. Macroporous strongly basic anion-exchange resin D261 offered the best separation performance of sinigrin, because of the highest adsorption and desorption capacity. The equilibrium experimental data of the adsorption of sinigrin on D261 resin at different temperatures fit better to the Freundlich model. The optimum parameters were obtained to ensure the high efficiency of separation. After treatment with D261 resin, the purity of sinigrin in the product was increased 15.57-fold from 3.75% to 58.37%, and the recovery of sinigrin was 79.82%. Furthermore, ELSD-HPLC, UV and IR applied to examine the effect of separation using macroporous ion-exchange resins supported the result that the D261 resins could separate and concentrate sinigrin from other impurities effectively, and the content of sinigrin was increased significantly. Therefore, it can be concluded that results in this study may provide scientific references for the sinigrin production from Indian mustard seeds.

ACKNOWLEDGEMENTS

The authors acknowledge the support of the Natural Science Foundation of China (20776009, 20976009) and (2008066005), and the Young Scholars Funds of Beijing University of Chemical Technology (QN.0809).

NOMENCLATURE

BV : bed volume
C_0 : the initial concentration of sinigrin in solution [mg/mL]
C_d : the concentration of sinigrin in the eluent [mg/mL]
C_e : the equilibrium concentration of sinigrin in solution [mg/mL]
D : the desorption ratio [%]
E : the adsorption ratio [%]
ESLD : evaporative light scattering detector
FTIR : fourier transform infrared
HPLC : high-performance liquid chromatography
IR : infrared
K : the adsorption equilibrium constant in Langmuir equation
K_f : the Freundlich constant
m_s : the mass of the resin [g]
1/n : the empirical constant in Freundlich constant
q_0 : the empirical constant in Langmuir equation
q_e : the adsorption capacity [mg/g]
TFA : trifluoroacetic acid
UV : ultraviolet
V : the volume of the sample solution [mL]
V_d : the volume of the eluete [mL]

REFERENCES

1. J. G. Michael, *Nutr.*, **24**, 393 (2008).
2. N. Rangkadilok, M. E. Nicolas, R. N. Bennett, R. R. Premier, D. R. Eagling and P. W. J. Taylor, *Sci. Hortic.*, **96**, 11 (2002).
3. J. W. Fahey, A. T. Zalcmann and P. Talalay, *Phytochemistry*, **56**, 5 (2001).
4. K. Isshiki, K. Tokuoka, R. Mori and S. Chiba, *Biosci., Biotechnol., Biochem.*, **56**, 1476 (1992).
5. C. M. Lin, J. F. Preston and C. I. Wei, *J. Food Prot.*, **63**, 727 (2000).
6. D. X. Hou, M. Fukuda, M. Fujii and Y. Fuke, *Cancer Lett.*, **161**, 195 (2000).
7. T. Nomura, S. Shinoda, T. Yamori, S. Sawaki, I. Nagata, K. Ryoyama and Y. Fuke, *Cancer Detect. Prev.*, **29**, 155 (2005).
8. C. Krul, C. Humblot, C. Philippe, M. Vermeulen, M. Vannuenen, R. Havenaar and S. Rabot, *Carcinogenesis*, **23**, 1009 (2002).
9. Q. Z. Du, J. Fang, S. J. Gao, Q. Y. Zeng and C. H. Mo, *Sep. Purif. Technol.*, **59**, 294 (2008).
10. N. Charpentier, S. Bostyn and J. P. Coïc, *Ind. Crops. Prod.*, **8**, 151 (1998).
11. J. W. Fahey, K. L. Wade, K. K. Stephenson and F. E. Chou, *J. Chromatogr. A*, **996**, 85 (2003).
12. S. Rochfort, D. Caridi, M. Stintion, T. V. Craige and R. Jones, *J. Chromatogr. A*, **1120**, 205 (2006).
13. A. Toribio, J. M. Nuzillard and J. H. Renault, *J. Chromatogr. A*, **1170**, 44 (2007).
14. C. Nobre, M. J. Santos, A. Dominguez, D. Torres, O. Rocha, A. M. Peres, I. Rocha, E. C. Ferreira, J. A. Teixeira and L. R. Rodrigues, *Anal. Chim. Acta*, **654**, 71 (2009).
15. S. Ou, Y. Luo, F. Xue, C. Huang, N. Zhang and Z. Liu, *J. Food Eng.*, **78**, 1298 (2007).
16. R. Kiefer and W. H. Höll, *Ind. Eng. Chem. Res.*, **40**, 4570 (2001).
17. S. Rengaraj, Y. Kim, C. K. Joo, K. Choi and J. Yi, *Korean J. Chem. Eng.*, **21**, 187 (2004).
18. T.-Y. Kim, S.-K. Park, S.-Y Cho, H.-B. Kim, Y. Kang, S.-D. Kim and S.-J. Kim, *Korean J. Chem. Eng.*, **22**, 91 (2005).
19. J. W. Lee, H. J. Jung and H. Moon, *Korean J. Chem. Eng.*, **14**, 277 (1997).
20. D. C. Sherrington, *Chem. Commun.*, **21**, 2275 (1998).
21. I. M. Abrams and J. R. Millar, *React. Funct. Polym.*, **35**, 7 (1997).
22. B. Q. Fu, J. Liu, H. Li, L. Li, F. S. C. Lee and X. R. Wang, *J. Chromatogr. A*, **1089**, 18 (2005).
23. N. Rangkadilok, M. E. Nicolas, R. N. Bennett, R. R. Premier, D. R. Eagling and P. W. J. Taylor, *Sci. Hortic.*, **96**, 27 (2002).
24. A. A. Zagorodni, D. L. Kotova and V. F. Selemenev, *React. Funct. Polym.*, **53**, 157 (2002).
25. L. A. Rodrigues and M. L. C. P. da Silva, *Desalination*, **263**, 29 (2010).
26. Y. Wang, H. Gao, R. Yeredla, H. Xu and M. Abrecht, *J. Colloid. Interf. Sci.*, **305**, 209 (2007).
27. E. M. Silva, D. R. Pompeu, Y. Larondelle and H. Rogez, *Sep. Puri. Technol.*, **53**, 274 (2007).

28. B. Zhang, R. Y. Yang, Y. Zhao and C. Z. Liu, *J. Chromatogr. B*, **867**, 253 (2008).
29. P. Baskaralingam, M. Pulikesi, D. Elango, V. Ramamurthi and S. Sivanesan, *J. Hazard. Mater. B*, **128**, 138 (2006).
30. M. W. Jung, K. H. Ahn, Y. H. Lee, K. P. Kim, R. P. Insook, J. S. Rhee, J. T. Park and K. J. Paeng, *J. Chromatogr. A*, **917**, 87 (2001).
31. R. E. Traybal, Mass Transfer Operation, Tata McGraw Hill, Singapore (1981).
32. P. Q. Kuang, H. Liang and Q. P. Yuan, *Sep. Sci. Technol.*, **46**, 179 (2011).